Effect of Chemical Kinetics in the Expansion Flow of a Rotating Detonation Engine

Douglas A. Schwer K. Kailasanath
Laboratories for Computational Physics and Fluid Dynamics
Naval Research Laboratory, Washington, DC, USA

1 Introduction

Rotating detonation engines (RDEs) represent a novel approach to using the high efficiency detonation thermal cycle without some of the drawbacks of the pulsed detonation engines (PDEs). Similar to the PDE, the RDE has the advantage of being operated over a wide range of conditions and Mach numbers. Unlike the PDE, it does not have to refill and initiate a detonation 20 to 100 times every second, it provides a steady source of thrust, and can scale up to larger thrust sizes easily, making it an attractive alternative to PDEs. The RDE does have its own set of technical challenges. Since the detonation wave continually runs near the head-end section of the combustion chamber, the inlet micro-nozzles can be subjected to intense pressures and temperatures, and may also be vulnerable to back flow into the premixture plenum. Conditions within the combustion chamber, too, are less well understood than conditions within a PDE, so that designing a combustion chamber to withstand the forces and heat-fluxes typical in an RDE may be more problematic.

Nevertheless, the feasibility of RDEs has been experimentally shown at the Lavrentyev Institute of Hydrodynamics [1], and several recent numerical [2,3] and experimental [4] studies have shown that the RDE is worth continued investigation. We have developed a code for simulating two-dimensional and three-dimensional RDE combustion chambers using the same algorithms that have been applied successfully to PDEs and for general detonation research [5-7]. In our previous papers [8-10], we have investigated several different aspects of hydrogen-air RDEs; including pressure effects and engine sizing, hydrocarbon fuels, as well as describing in more detail the features of the flow field.

The present paper extends the current hydrogen-air model to consider chemistry in the expansion flow of the RDE. We use our previous work on hydrocarbon fuels [9] for a more accurate representation of the thermodynamics, and add non-equilibrium kinetics to represent the chemistry that occurs as the flow expands and cools and recombination takes place.

2 Rotating Detonation Engine Model

A basic RDE is shown in Figure 1, with the main features identified in the "unrolled" temperature solution. The combustion chamber is an annular ring, where the mean direction of flow is from the head end (bottom in figure) to the exit plane (top). The micro-injectors flow in a premixture of fuel and air or oxygen, and a detonation propagates circumferentially around the combustion chamber consuming the freshly injected mixture. The gas then expands azimuthally and axially, and can be either subsonic or supersonic (or both), depending on the back pressure at the outlet plane. The flow has a very strong circumferential aspect due to the detonation wave propagation. Because the radial dimension is typically small compared to the azimuthal and axial dimension, there is generally little variation radially within the flow field. Because of this, the RDE is usually "unrolled" into two dimensions, and we do this for our simulations with small thickness to diameter ratios. The main features of an RDE have been discussed previously in our papers [8, 10] and have also been discussed by others [3].

The focus of this paper is on the flow field within an RDE combustion chamber. For the two-dimensional simulations, the azimuthal direction is *x*, and the axial direction is *y*. The RDE model follows the Euler model developed in Ref. 8 closely, with some important differences. The conservation equations to be solved are the standard Euler equations, with additional conservation equations for species,

$$\frac{\partial n_i}{\partial t} + \nabla \cdot n_i \mathbf{v} = -\dot{w}_{\mathrm{det}} - \dot{w}_{\mathrm{exp}} \tag{1}$$

where the solution variables are density, ρ, momentum, $\rho\mathbf{v}$, total energy, E, and species concentration, n_i. For this paper, we use 6th order polynomial curve-fits in temperature for species enthalpy and the ideal gas law to calculate the pressure P from total energy E and species concentration n_i, as described in detail in Ref. 9.

2.1 Detonation Chemistry

The chemical terms in the species and energy equation are divided into two terms, a detonation chemistry term, and an expansion flow chemical term. For this study, the detonation reaction rate term is calculated through an induction parameter model [9]. For the induction parameter model, we convect an additional induction variable, τ, with a source term dependent on the induction time:

$$\frac{\partial \tau}{\partial t} + \nabla \cdot \tau\mathbf{v} = \rho / t_{\mathrm{ind}} \tag{1}$$

In regions where $\tau / \rho > 1$, reactant is converted to products and heat is released. Care must be taken to spread the heat release out over several time-steps so that the numerical scheme remains stable. For previous simulations, we considered two-species models for the detonation wave, a reactant and a product species. The reactant species is simply a combination of the fuel and air based on the equivalence ratio of the premixture. In previous simulations, the product species are obtained by running a chemical equilibrium code such as CEA2 [11], and combining the equilibrium species into one effective product species. For this work, however, in addition to a reactant species, we also track each product species with separate conservation equations, allowing us to incorporate additional chemical kinetics in the expansion region. Thus, for the H2/Air systems that we are considering, we convect 11 species: Reactant (approx. 30% H2, 15% O2, and 55% N2 for stoichiometric H2/Air), H2, O2, H2O, OH, H, O, HO2, H2O2, N2, and NO. The reactants and product mole fractions produced from the CEA2 code are given in Table 1.

2.2 Expansion Region Chemistry

In the expansion region, we incorporate an elementary kinetic mechanism that represents the detailed chemistry as the flow expands and cools. For the hydrogen/oxygen chemistry, we use a kinetic mechanism from Saxena and Williams [12]. The 12-step H2/O2 mechanism is a subset of a larger mechanism that includes hydrocarbons up to propane. Because the expansion region is typically at a much lower pressure than CJ pressure (5 atm compared to 40 atm), extreme high pressure reactions important to the detonation kinetics are only minimally important for the expansion region. The complete mechanism is described in Table 2. The current work does not include nitrogen chemistry, however, in future work we plan to include nitrogen chemistry to examine pollutant concentrations in the exhaust.

2.3 Solution Procedure

The solution procedure is based on the FCT-algorithm [13] and domain decomposition for the parallelism. The induction parameter model is based on previous work on pulsed detonation engines [14], and the procedure and convergence criteria used for RDEs has been detailed in Ref. 8. The detailed kinetic mechanism for the expansion flow chemistry is computed using the Chemeq2 ODE solver [15], which we have found to work very well for CFD simulations.

3 RDE Flow-Field with Kinetics in Expansion Region

The simulations were computed using a baseline geometry developed in our previous studies and described in Ref. 9. The annular combustion chamber has an inner and outer diameter of 8 and 10 cm, resulting in an average azimuthal length of 28.27 cm. The axial length is set to 10 cm. The area ratio for the injection system is set at 0.2. The stagnation injection conditions are a stoichiometric mixture of hydrogen/air at 10 atm and 300 K and the exhaust back pressure is 1 atm. Two cases are run for this abstract, one with expansion flow kinetics and one without.

Comparison of the overall flow-field features between the simulations with and without expansion flow chemistry showed no significant difference with the addition of kinetics. Figure 2 shows the mole fraction for both the OH and H radicals in the expansion region. As the flow expands, the hydrogen and OH radicals combine to form additional H2O. Due to the high temperatures in the slip region (as shown in Fig. 1, feature (C)), the amount of radicals is highest in this region, and is actually higher than the CJ equilibrium values found in Table 1. The high temperatures in this region are due to deflagration reactions at the boundary of the fill region (E) being compressed by the oblique shock wave (B). Figure 3 shows averaged temperature, pressure, and selected species mole fractions at the exhaust plane. With exhaust kinetics, the pressure is uniformly higher throughout the exhaust plane, due to the higher temperatures in most of the expansion flow, and higher radical concentrations in the slip region. Examining the radical species, they are considerably lower with expansion flow kinetics for all of the species, and H2O has a significantly higher mole-fraction over the entire exhaust plane.

Integrating the mass flow and thrust force at the exhaust plane over the entire averaging run, we obtain an averaged specific impulse of 5000 s and 4940 s with and without expansion flow kinetics respectively. Interestingly, the main difference was the mass flow rate, with the mass flow rate with the expansion flow kinetics being slightly lower. For both cases, the detonation velocity was close 1820 m/s.

4 Conclusion

The results show that including expansion flow chemistry has only a small effect on the overall flow features within an RDE; however, radical concentrations are significantly different at the exhaust plane.

The performance of a baseline hydrogen/air RDE increased by 60 s with expansion flow chemistry, due to recombination of radicals and more production of H2O resulting in additional heat release. Further work to include nitrogen chemistry in the expansion flow will help determine the amount of pollutant emissions that can be expected from RDEs running at various operating conditions.

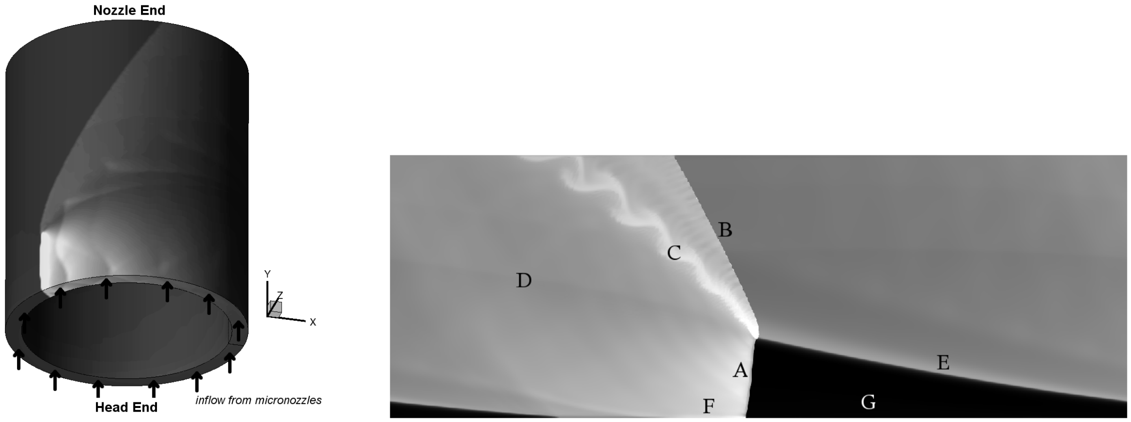

Figure 1. Sample three-dimensional simulation of an RDE showing pressure (left) and temperature (right) solutions. The temperature solution is unrolled to show different flow-field features for the RDE. A) detonation wave, B) leading-edge shock wave, C) slip line between detonated and non-detonated products, D) expansion region for detonation products, E) non-detonated products from injection and diffusion, F) blocked micro-injectors, G) choked micro-injectors. P_{st}=10 atm, T_{st}=300 K, L=10 cm, l = 28.27 cm, a=0.2.

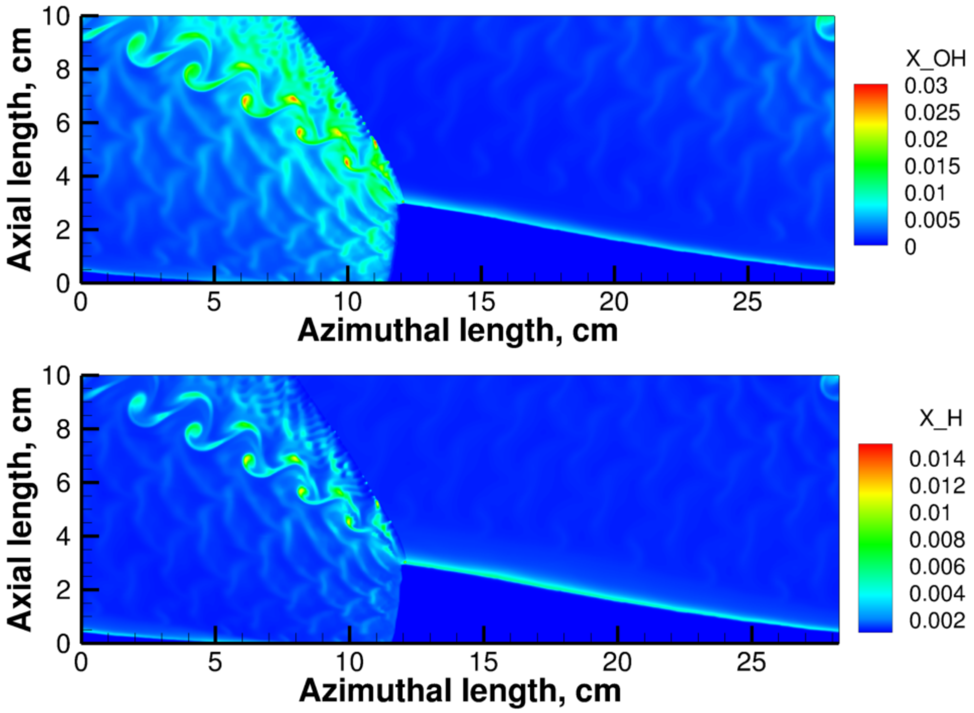

Figure 2. Mole-fraction of OH (top) and H (bottom) with expansion flow kinetics. Same conditions as Fig. 1.

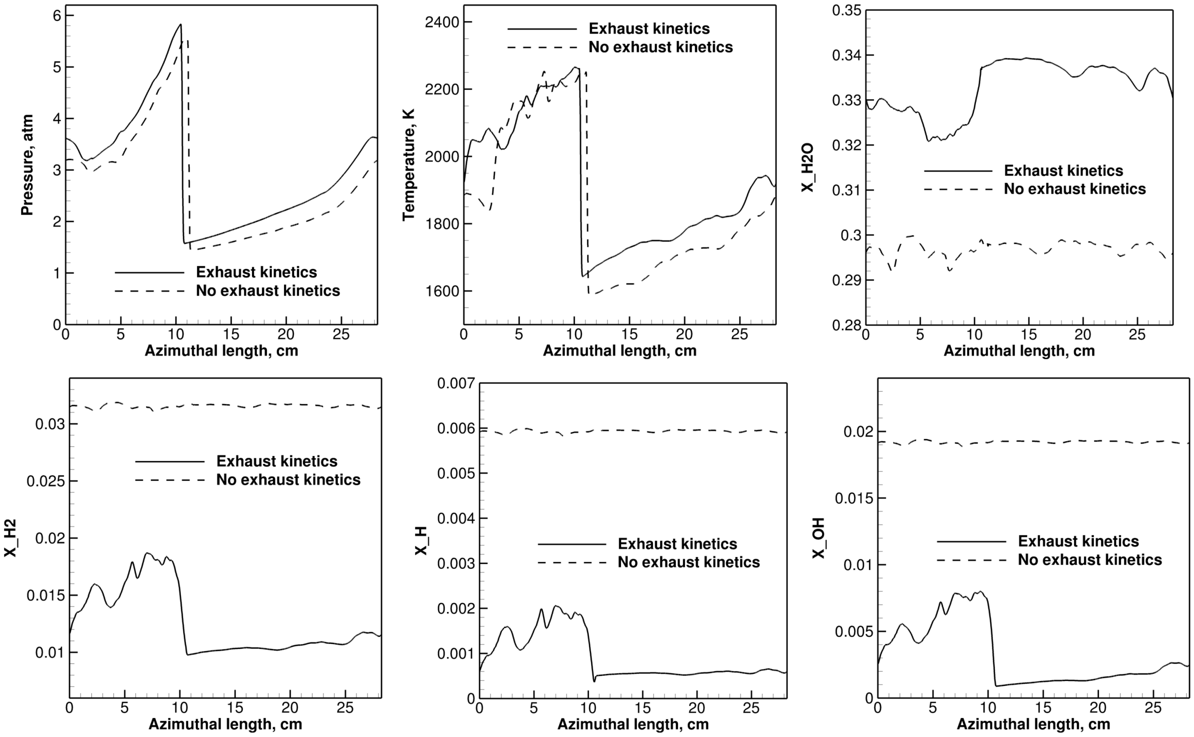

Figure 3. Mole-fractions of important species, temperature and pressure, at the exhaust plane of the RDE, axial location *y*=10 cm. Same conditions as Fig. 1.

Table 1: Products of H2/O2/N2 detonation from CEA2 equilibrium code.

Property or species mole fraction	Reactant conditions	CJ Product conditions
Pressure	1.013 atm	15.570 atm
Temperature	300 K	2942.22 K
X_H2	0.29585799	0.03130031
X_O2	0.14792899	0.00756008
X_H2O	0.0	0.29449294
X_OH	0.0	0.01904019
X_H	0.0	0.00588006
X_O	0.0	0.00202002
X_HO2	0.0	0.0001000
X_NO	0.0	0.00755008
X_N2	0.55621302	0.63214632

Table 2: Kinetic mechanism used for expansion flow in an H2/Air Rotating Detonation Engine.

```
 H+O2=OH+O            3.52E+16   -0.7     71420.   ! 1F
   REV /              7.04E+13   -0.26      600. / ! 1B
H2+O=OH+H             5.06E+04    2.67    26320.   ! 2F
   REV /              3.03E+04    2.63    20230. / ! 2B
H2+OH=H2O+H           1.17E+09    1.3     15210.   ! 3F
   REV /              1.28E+10    1.19    78250. / ! 3B
H+O2(+M)=>HO2(+M)     4.65E+12    0.44        0.   ! 4F
   LOW /              5.75E+19   -1.4         0. /
   TROE / 0.5 1.E+30 1.E-30 /
   H2/2.5/ H2O/16.0/
HO2+H=>OH+OH          7.08E+13    0.0      1230.   ! 5F
HO2+H=H2+O2           1.66E+13    0.0      3440.   ! 6F
   REV /              2.69E+12    0.36   231860. / ! 6B
HO2+OH=>H2O+O2        2.89E+13    0.0     -2080.   ! 7F
H+OH+M=H2O+M          4.00E+22   -2.0         0.   ! 8F
   REV /              1.03E+23   -1.75   496140. / ! 8B
   H2/2.5/ H2O/12.0/
H+H+M=H2+M            1.30E+18   -1.0         0.   ! 9F
   REV /              3.04E+17   -0.65   433090. / ! 9B
   H2/2.5/ H2O/12.0/
HO2+HO2=>H2O2+O2      3.02E+12    0.0      5800.   ! 10F
HO2+H2=>H2O2+H        1.62E+11    0.61   100140.   ! 11F
H2O2(+M)=>2OH(+M)     2.62E+19   -1.39   214740.   ! 12F
   LOW /              8.15E+23   -1.9    207620. /
   TROE / 0.735 94.0 1756.0 5182.0 /
   H2/2.5/ H2O/6.0/
```

References

[1] Bykovskii, F.A., Zhdan, S.A., and Vedernikov, E.F. “Continuous spin detonations,” *Journal Propulsion and Power*, Vol. 22, pp 1204, 2006.

[2] Zhdan, S.A., Bykovskii, F.A., and Vedernikov, E.F. “Mathematical Modeling of a Rotating Detonation Wave in a Hydrogen-Oxygen Mixture,” *Combustion, Explosion, and Shock Waves,* Vol. 43, No. 4, pp. 449, 2007.

[3] Hishida, M., Fujiwara, T., and Wolanski, P. “Fundamentals of rotating detonation engines,” *Shock Waves*, Vol. 19, No. 1, pp. 1-10, 2009.

[4] Kindracki, J., Wolanski, P., and Gut, Z. “Experimental research on the rotating detonation in gaseous fuels-oxygen mixtures,” *Shock Waves*, Vol. 21, pp 75-84, 2011.

[5] Kailasanath, K., Oran, E.S., Boris, J.P., and Young, T.R., ‘‘Determination of detonation cell size and the role of transverse waves in two-dimensional detonations," *Combust Flame*, Vol. 61, No. 3, pp 199-209, 1985.

[6] Kailasanath, K. and Patnaik, G. ‘‘Performance estimates of pulsed detonation engines," *Proc Combust Inst*, Vol. 28, pp 595-601, 2000.

[7] Kailasanath, K., Patnaik, G., and Li, C. ‘‘On factors controlling the performance of pulsed detonation engines," in *High-speed deflagration and detonation: Fundamentals and control*. Eds: G. Roy, S. Frolov, D. Netzer, and A. Borisov, Moscow, Russia: Enas Publ. 193-206, 2001.

[8] Schwer, D.A. and Kailasanath, K. ‘‘Numerical investigation of the physics of rotating detonation engines," *Proc Combust Inst*, Vol. 33, p 2195, 2011.

[9] Schwer, D.A., and Kailasanath, K. “Fluid Dynamics of Rotating Detonation Engines with Hydrogen and Hydrocarbon Fuels,” *Proc Combust Inst*, Vol. 34, pp 1991-1998, 2013.

[10] Nordeen, C.A., Schwer, D.A., Schauer, F., Hoke, J., Cetegen, B. and Barber, T. “Thermodynamic Modeling of a Rotating Detonation Engine,” AIAA Paper 2011-803, 49th AIAA Aerospace Sciences Meeting, 2011.

[11] Gordon, S. and McBride, B.J. *Computer Program for Calculation of Complex Chemical Equilibrium Compositions and Applications*, NASA Reference Publication 1311, 1994.

[12] Saxena, P. and Williams, F.A. “Testing a small detailed chemical-kinetic mechanism for the combustion of hydrogen and carbon monoxide,” *Combust Flame*, Vol 145, pp 316-323, 2006.

[13] Boris, J.P. and Book, D.L. ‘‘Flux Corrected Transport I. SHASTA, A fluid transport algorithm that works," *J Comput Phys*, Vol. 11, No. 3, p 38, 1973.

[14] Li, C., Kailasanath, K., and Oran, E.S. ‘‘Detonation structure behind oblique shocks," *Phys. Fluids*, Vol. 6, No. 4, pp 1600-1611, 1994.

[15] Mott, D.R., Oran, E.S., and van Leer, B. *J Comput Phys*, Vol. 164, No. 2, p 407, 2000.